PHYSICAL REVIEW B

CONDENSED MATTER

THIRD SERIES, VOLUME 40, NUMBER 16 1 DECEMBER 1989

Desorption of positive oxygen ions induced by keV heavy-ion bombardment of transition metals with adsorbed O_2 and CO

Michael G. Kaurin*
A. W. Wright Nuclear Structure Laboratory, Yale University, New Haven, Connecticut 06511

Robert A. Weller
A. W. Wright Nuclear Structure Laboratory, Yale University, New Haven, Connecticut 06511
and Department of Materials Science and Engineering, Vanderbilt University, Nashville, Tennessee 37235
(Received 9 March 1989; revised manuscript received 31 July 1989)

We report measurements of O^+ secondary-ion emission induced by 25–250-keV Ne^+, Ar^+, and Kr^+ bombardment of oxidized surfaces of Ti, Mo, Nb, W, and Ni, and of Ni and Pd surfaces with adsorbed CO. The yield $I(O^+)$ of O^+ from bombardment of oxygen adsorbed onto nickel, as well as the yields of all metal and metal-oxide ions, exhibits behavior similar to the sputtering yields as functions of incident ion energy. By contrast, the yield of O^+ from the other oxidized targets increases linearly with projectile velocity v, making $dI(O^+)/dv$ a convenient, velocity-independent parameter with which to characterize the emission. The variation of $dI(O^+)/dv$ with projectile species depends on the substrate. For Ti and, to a lesser extent, Nb, $dI(O^+)/dv$ is independent of projectile species, although for Mo and W $dI(O^+)/dv$ varies with projectile species in a manner similar to the corresponding variation of the electronic stopping power of the projectile. However, the magnitude of the observed O^+ yields is not consistent with that expected if the O^+ emission is produced by secondary-electron-stimulated desorption. $I(O^+)$ for bombardment of Ni and Pd surfaces with adsorbed CO is not clearly related to either the sputtering yield or the O^+ yields from the oxidized targets.

I. INTRODUCTION

Sputtered ions generally receive their momentum either from participation in a collision cascade or from a direct collision with an incident beam ion. In the former case, the ionization probability, which is determined by various electronic interactions with neighboring atoms and the surface, is experimentally observed to have an inverse exponential dependence on the ionization potential of the sputtered atom.[1–6] Williams,[7] however, has observed the emission of F^+ from fluorinated silicon under ion bombardment and found that the energy distribution was inconsistent with that expected from a collision cascade. Since the F^+ yield as a function of beam velocity was similar to that of the silicon LVV Auger electrons, Williams concluded that these Auger electrons, by creating core holes in fluorine atoms, were leading to the desorption of F^+ via the Knotek-Feibelman mechanism of electronically stimulated desorption (ESD).[8]

More recently, O'Connor, Blauner, and Weller[9,10] observed unexpectedly large yields of electronegative ions from metals under MeV ion bombardment. The dependence of these yields on beam energy differed from that of the sputtered metal ion yields. Also, Blauner and Weller[11–13] observed O^+ yields for 15–275-keV noble-gas ion bombardment of oxidized aluminum and vanadium surfaces which increased linearly with beam velocity. This was in contrast to their measured yields of metal ions, whose dependence on beam energy was consistent with models of ionization that invoke atomic collisions or collision cascades. Noting the linear dependence on beam velocity of the electronic stopping power and the secondary electron yield for the range of beam energies used, Blauner and Weller proposed that the O^+ emission resulted from electronic processes induced by the incident ions; in particular, desorption stimulated by secondary electrons was suggested.[11] Indeed, the O^+ yields from aluminum for the various beams, as functions of beam velocity, were closer to lying on a common curve when divided by the constant of proportionality between Lindhard's electronic stopping power and beam velocity (to remove the dependence of the yields on beam species expected for emission arising from electronic processes).[12] However, Blauner and Weller also found that the O^+

yields for vanadium were simply proportional to beam velocity with no additional dependence on the beam species, apparently precluding an emission mechanism common to these two targets.[11]

In these experiments, we have extended the work of Blauner and Weller by investigating the beam-velocity and beam-atomic-number dependences of the O^+ yields during 25–250 keV Ne^+, Ar^+, and Kr^+ bombardment of other oxidized transition metal surfaces (Ti, Nb, Mo, and W) in an attempt to discover whether the simple velocity dependence of the O^+ yields for oxidized vanadium is a general phenomenon for transition metals, or the result of some coincidental cancellation of factors. That these metals preferentially form maximally valent oxides is important for the operation of the Knotek-Feibelman mechanism of ESD.[8] Since the necessity of maximal valency for ESD is disputed, however,[14–18] we have also examined the secondary-ion emission from oxygen adsorbed onto surfaces of nickel, which does not form a maximally valent oxide,[8] but has been observed to yield O^+ in ESD experiments.[16–18] In addition, we shall discuss the possible role played by secondary electrons in the emission of O^+ from these targets by examining whether our observed O^+ yields are consistent with observed ESD cross sections and secondary electron yields for transition metals. We shall also consider the role of projectile Auger electrons.

Finally, we report on studies of the emission of O^+ from carbon monoxide adsorbed onto nickel and palladium surfaces. For these metals, CO adsorbs molecularly,[19,20] with the carbon atom bonding directly to the metal and the oxygen atom bonding directly only to the carbon atom.[20] Therefore, in contrast to the situation for O_2 adsorption, in the case of CO adsorption the oxygen bonding is covalent rather than ionic. Although ionic bonding with maximal valency is necessary for the occurrence of the Knotek-Feibelman mechanism,[8,21] other workers[22] have observed ESD of O^+ from CO-adsorbed metal surfaces. Therefore, we have investigated this system to determine the effect of the type of bond on the O^+ emission during ion bombardment.

II. EXPERIMENTAL

The experimental procedure followed was essentially that of Blauner and Weller.[1] Polycrystalline targets of 99.95% pure Ti, Nb, Mo, W, Ni, and Pd with thickness 0.127–0.25 mm were degreased in Freon TF and mounted in a UHV chamber, which was then baked at 100 °C for 1–2 days. The ultimate chamber pressure was about 2×10^{-10} Torr, with the pressure remaining below 3×10^{-10} Torr with all of the valves open between the chamber and the accelerator. The targets were sputter cleaned with 200 keV Ar^+ beams rastered over 1 cm^2 for a total incident charge of 0.4–1.0 Coulomb. This was estimated to remove 2000 to 15 000 monolayers of target material.[23] The cleanliness of the targets was verified by examination of their secondary-ion mass spectra. After the sputter cleaning, the targets were exposed to 1×10^{-6} Torr of 99.99% pure gas for 1000 s (O_2) or 2000 s (CO), the gases being admitted through separate leak valves. We did not attempt to determine the concentration of the adsorbates on the surfaces or the stoichiometry of the oxides formed. A residual pressure of 5×10^{-8} Torr of the adsorbate gas was maintained in the chamber throughout the ion yield measurements.

The prepared targets were bombarded by momentum-analyzed 25–250 keV beams of Ne^+, Ar^+, and Kr^+, rastered and collimated to form a beam spot of area 0.09 cm^2, and incident on the target at an angle of 30° from the target normal. Typical beam currents ranged from 0.5 nA to 1.0 nA; this avoided significant target damage during the measurements. Repeated measurements using 200 keV Ar^+ beams were made throughout each run to verify the constancy of the surface and to provide the basis for normalizing the data for day-to-day variations in the experimental conditions. The secondary ions were analyzed by a quadrupole mass spectrometer equipped with an electrostatic energy prefilter which allowed ions with energy 4–6 eV to enter the quadrupole.[13] (We show

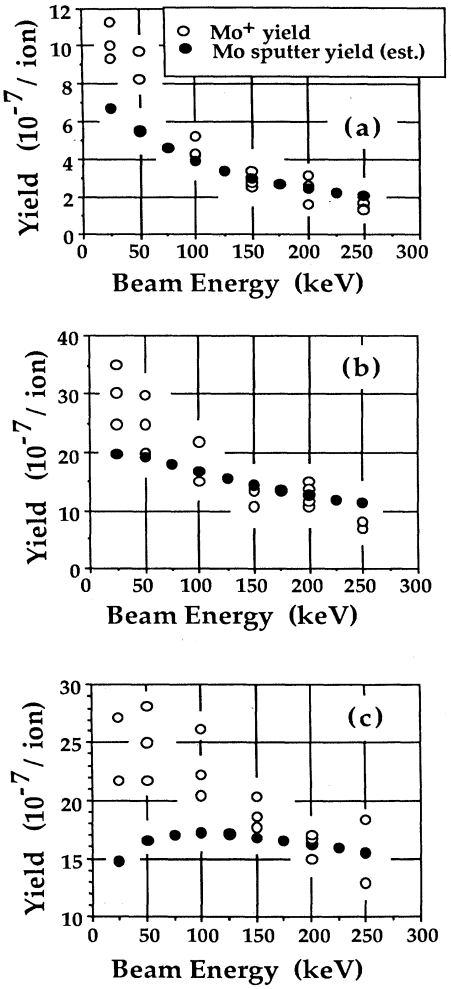

FIG. 1. Measured yields of Mo^+ (open circles), and Mo sputtering yields (solid circles) calculated as in Ref. 25 and normalized to the measured Mo^+ yields at 200 keV, for bombardment of O/Mo by 25–250 keV (a) Ne^+; (b) Ar^+; (c) Kr^+.

in the following that this limited energy range does not introduce significant systematic error into our results.) The quadrupole axis was perpendicular to the target surface.

Incoming counts from the secondary ions passed by the quadrupole mass spectrometer were stored in a multichannel analyzer (MCA) operated in the multichannel scalar mode. Both the mass spectrometer and the MCA were controlled by a computer; the mass of the ions allowed through the mass spectrometer was linearly related to the MCA channel number. Secondary-ion yields were measured at single channels located at the peaks of the masses of interest (three channels were used for O^+ from the Ni and Pd targets). Data were collected for a preset amount of incident beam charge per MCA channel (typically 5 nC).

The circuit for the measurement of beam current included the target and a Faraday cage which surrounded the target to collect secondary electrons. Later beam current measurements, independent of the secondary-ion yield measurements, included the quadrupole prefilter in the circuit to allow correction of the results for secondary electrons hitting the prefilter. We made additional measurements of the current from the target alone to estimate the secondary-electron yields, for comparison of their dependence on beam velocity with that of the O^+ yields.

Secondary-electron energy distributions were measured for 25–200 keV Ar^+ bombardment of a V target with adsorbed O_2, prepared in the same fashion as the other targets. We acquired integral energy distributions using a cylindrical mirror analyzer (Physical Electronics model 10-155) with the detector electronics set up for pulse counting. Under computer control, the analyzer swept

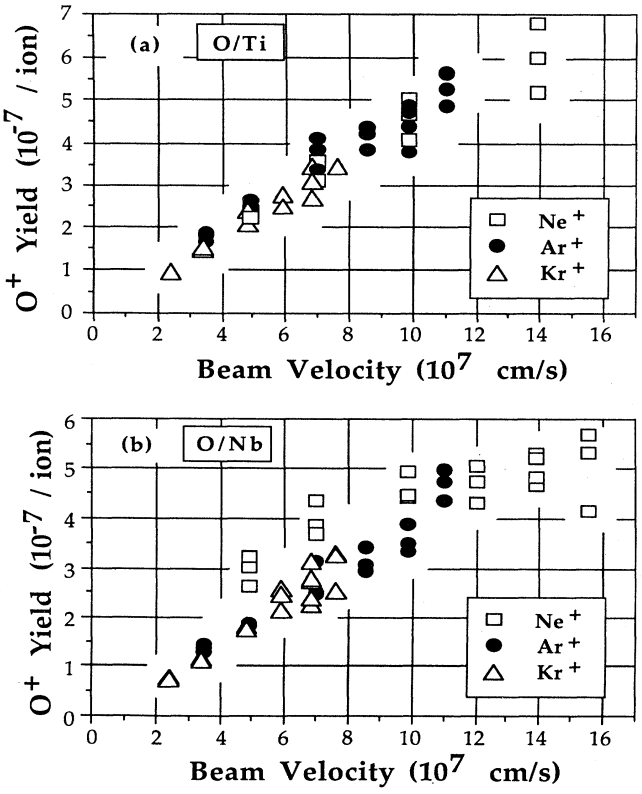

FIG. 2. O^+ yields per incident ion from 25–250 keV Ne^+, Ar^+, and Kr^+ bombardment of (a) O/Ti; (b) O/Nb.

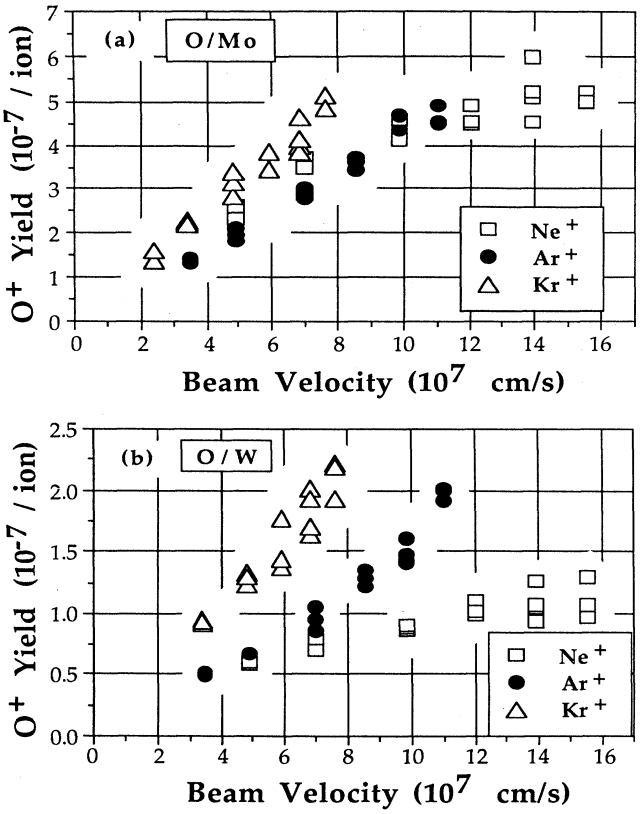

FIG. 3. O^+ yields per incident ion from 25–250 keV Ne^+, Ar^+, and Kr^+ bombardment of (a) O/Mo; (b) O/W.

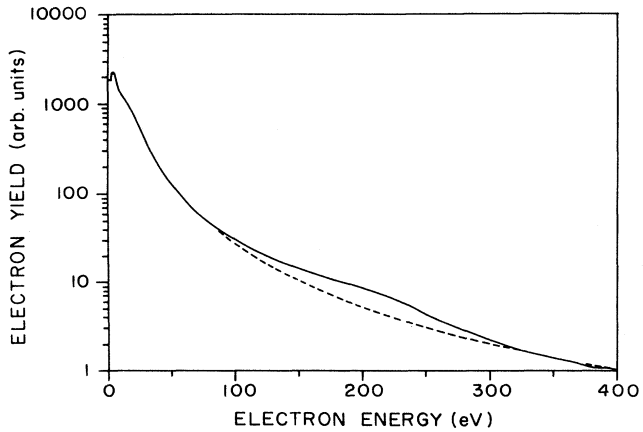

FIG. 4. Unnormalized energy distribution of secondary electrons emitted from O/V during 200-keV Ar^+ bombardment. The dashed line indicates the background of secondary electrons under the Auger feature.

through a range of electron energies of 0–2000 eV. The analyzer was at an angle of 90° with respect to the ion beam. The target normal was at an angle of 55° with respect to the beam, resulting in a beam spot large compared with the field of view of the analyzer,[24] so that the energy resolution was not optimal.

III. RESULTS

Our measured yields of Mo^+ as a function of beam energy for bombardment of O_2 adsorbed onto Mo (denoted O/Mo) are shown in Fig. 1 for all three beams, together with the sputtering yields calculated using the semiempirical expression of Matsunami *et al.*[23] and scaled to equal the ion yields at 200 keV. The behavior of all other metal and metal-oxide ion yields is similar to that of Mo^+. As shown in Fig. 1, the measured secondary-ion yields exhibit a stronger dependence on beam energy than do the calculated sputtering yields, especially for the heavier beams. The ratios of the measured metal secondary-ion yields to the calculated sputtering yields (at 200 keV) ranged from $1-2\times10^{-8}$ for W to $6-12\times10^{-6}$ for Ti. These ratios have not been adjusted for the transmission of the energy prefilter and the quadrupole mass spectrometer. Comparing these ratios with the ionization probabilities found by Benninghoven[25] (0.4 for Ti^+ and 0.035 for W^+) and considering the decrease in the transmission of a quadrupole mass spectrometer with increasing ion mass,[26,27] we find that the transmission of our instrument is of the order $10^{-6}-10^{-5}$. It must be noted, however, that the energy distribution of sputtered Ti^+ has a maximum at about 10 eV,[28] as compared to the 4–6 eV energy range of our prefilter; this implies that the transmission for ions having an energy within our energy range is probably larger than calculated.

In Figs. 2 and 3 we present the yields of O^+ from ion bombardment of the Ti, Nb, Mo, and W targets as functions of beam velocity. As Blauner and Weller found for Al and V,[11–13] for our targets there is a clear difference between the behavior of the metal ion yields as functions of beam energy and that of the oxygen ion yields. The O^+ yields increase linearly with beam velocity for each beam species; we found this to be true for the measured secondary-electron yields also. The parameters from linear fits to the data are presented in Table I. These parameters, and the data presented in Figs. 2 and 3, suggest that the O^+ yields from bombardment of O/Ti and O/Nb are both independent of beam species, although the yields from Ne^+ bombardment of O/Nb are some-

TABLE I. Slopes and y intercepts computed by least-squares fit to the O^+ yields as linear functions of incident ion velocity, and slopes of the secondary electron yields, for 25–250 keV noble ion bombardment of oxidized transition metal surfaces. For the O^+ yields, units are 10^{-7} per ion, while for the secondary electron yields, units are per ion; in both cases, velocity units are 10^7 cm/s.

		O^+ Yields		Electron yields
Target	Beam	Slope	y intercept	Slope
Ti	Ne^+	0.40 ±0.05	0.48 ±0.49	0.19 ±0.03
	Ar^+	0.44 ±0.05	0.40 ±0.27	0.40 ±0.04
	Kr^+	0.46 ±0.05	0.03 ±0.19	0.61 ±0.07
Mo	Ne^+	0.26 ±0.03	1.5 ±0.3	0.26 ±0.02
	Ar^+	0.46 ±0.03	−0.26 ±0.12	0.44 ±0.03
	Kr^+	0.62 ±0.04	0.06 ±0.19	0.59 ±0.04
Nb	Ne^+	0.15 ±0.03	2.0 ±0.3	0.27 ±0.02
	Ar^+	0.41 ±0.05	−0.13 ±0.22	0.58 ±0.07
	Kr^+	0.41 ±0.03	0.28 ±0.15	0.68 ±0.04
W	Ne^+	0.049 ±0.004	0.39 ±0.05	0.22 ±0.01
	Ar^+	0.18 ±0.01	−0.24 ±0.06	0.42 ±0.02
	Kr^+	0.28 ±0.03	0.004 ±0.152	0.47 ±0.05

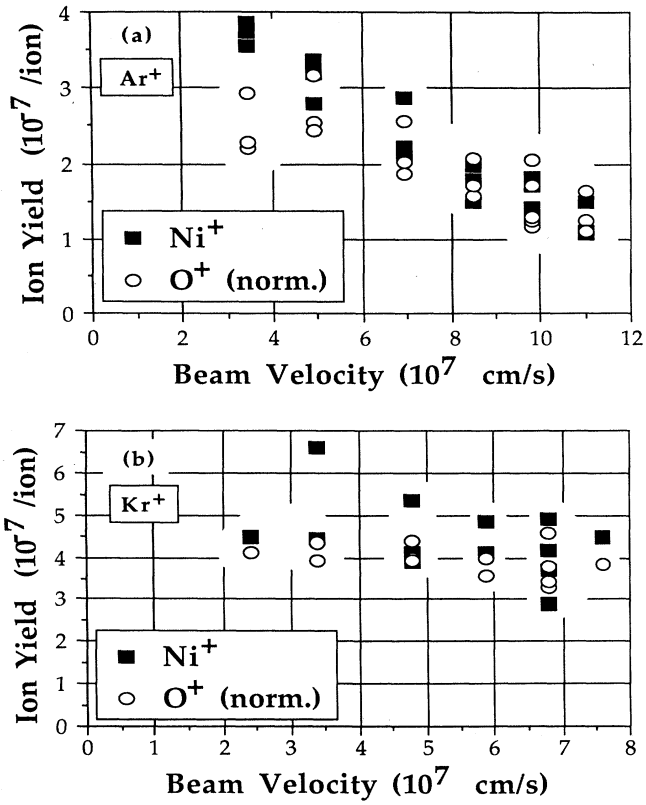

FIG. 5. Yields of Ni^+ and O^+ (normalized to the Ni^+ yield at 200 keV) from bombardment of O/Ni by 25–250 keV (a) Ar^+ (O^+ multiplied by 32.5); (b) Kr^+ (O^+ multiplied by 15.1).

what anomalous. Similarities also exist between the behaviors of the yields from bombardment of O/Mo and O/W, with both being dependent on beam species; again, the Ne^+ beams are a special case.

Figure 4 shows the (unnormalized) secondary electron energy distribution measured for 200 keV Ar^+ bombardment of O/V. The broad feature at around 200 eV shows the presence of Ar Auger electrons,[29] raising the possibility that the projectile Auger electrons could play a role in the emission of O^+.

Figure 5 shows the yields of O^+ and Ni^+ from ion bombardment of oxidized nickel. The O^+ yields have been scaled to equal the Ni^+ yields at 200 keV. The behavior of the O^+ yields is similar to that of the Ni^+ yields, indicating that, for this system, the O^+ desorption is produced by collision cascades. This behavior is in sharp contrast to that of the O^+ yields from bombardment of the other oxidized metal surfaces which were studied. Comparison of the scale of Fig. 2(a) with that of Fig. 5(a) (taking into account the scaling of the O^+ yields in the latter figure) shows that the yield of O^+ from ion bombardment of O/Ni is less than 1% of the yield of O^+ from bombardment of O/Ti.

The difference between O_2 adsorption and CO adsorption may be seen by comparing Figs. 5 and 6, the latter showing the yields of O^+ as functions of beam velocity for ion bombardment of CO/Ni and CO/Pd. In both cases, the O^+ yields do not follow the sputtering yields as functions of beam velocity, unlike the case for O_2 adsorbed onto nickel. In addition, the O^+ yields for bombardment of CO-adsorbed targets do not increase monotonically with projectile velocity, unlike the yields for bombardment of O/Ti, O/Nb, O/Mo, and O/W, although the O^+ yields for CO adsorption are within an order of magnitude of those for O_2 adsorption (excepting O/Ni).

In Fig. 7(a) we show the yields of CO^+ and Ni^+ from Ar^+ bombardment of CO/Ni, with the CO^+ yields scaled to equal the Ni^+ yield at 200 keV. Figure 7(b) presents the equivalent information for Ar^+ bombardment of CO/Pd. The data presented in these figures suggest that CO^+ emission from these targets is produced by collision cascades.

Finally, in Fig. 8 we present the yields of Ni^+ for O_2 and for CO adsorbed (separately) onto Ni; the results for O_2 adsorption have been normalized to those for CO adsorption at 200 keV. The behaviors of the Ni^+ yields for the two adsorbates are similar, with both being approximately proportional to the sputtering yield. The measured ionization probability of Ni for the CO-adsorbed target is larger than that for the O_2-adsorbed target by an order of magnitude; this extra enhancement of the Ni^+ yield has been observed previously by Winograd.[30]

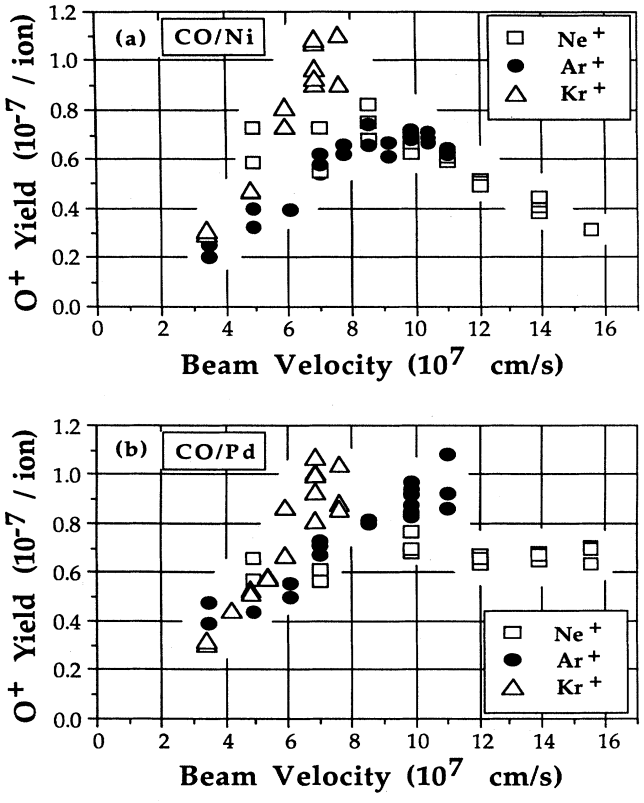

FIG. 6. O^+ yields from 25–250 keV Ne^+, Ar^+, and Kr^+ bombardment of (a) CO/Ni; (b) CO/Pd.

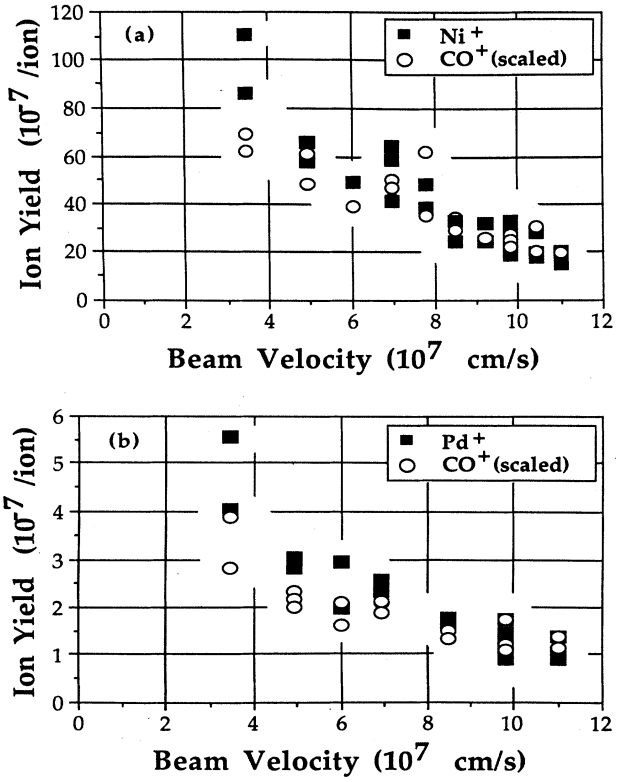

FIG. 7. Yields from bombardment by 25–250 keV Ar^+. (a) Ni^+ and CO^+ from CO/Ni (CO^+ multiplied by 324); (b) Pd^+ and CO^+ from CO/Pd (CO^+ multiplied by 12.8).

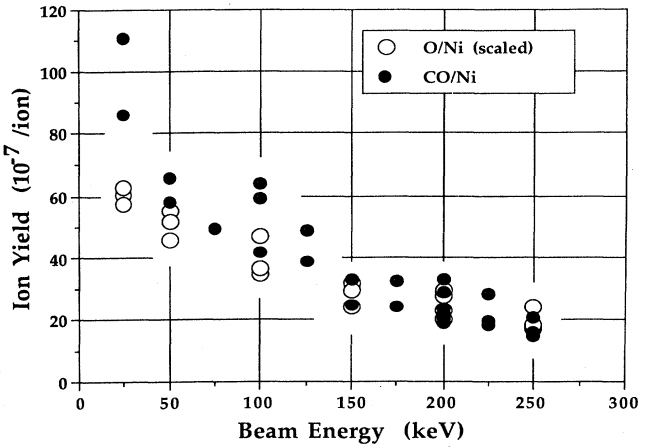

FIG. 8. Yields of Ni^+ from 25–250 KeV Ar^+ bombardment of O/Ni and CO/Ni (yields from O/Ni multiplied by 12.5).

IV. DISCUSSION

Figures 2, 3, 5, and 6 show that the functional dependence of the O^+ yield, $I(O^+)$, on beam velocity v is not the same for all adsorbate/substrate combinations studied. We shall first discuss the results for O_2 adsorption onto each metal. Our discussion will center on the proposal[11] that the emission of O^+ is caused by secondary electrons via ESD; we shall focus on the dependence of $I(O^+)$ on beam species and compare that dependence to the dependences of the secondary-electron yields and the electronic stopping powers on beam species. We shall also consider the consistency of our yields with observed ESD yields, and the possible role of projectile Auger electrons. Finally, we shall discuss the results for CO adsorption and compare them with the results for O_2 adsorption.

A. O_2 adsorption

As shown in Fig. 2(a) and Table I, the *combined* O^+ yields from bombardment of O/Ti are collinear for all three beams as functions of beam velocity; thus, $I(O^+)$ for bombardment of O/Ti is a function of the projectile velocity alone, with no additional dependence on projectile species. This result is in agreement with the result of Blauner and Weller for ion bombardment of O/V,[11] confirming that the collinearity is not coincidental or limited to the O/V system. It bears noting that, although Ti and V are not in the same column of the periodic table, they are in neighboring columns in the same row.

Although the linear dependence on projectile velocity of the O^+ yields from ion bombardment of O/Ti and O/V suggests the presence of electronic processes, the lack of dependence on beam species argues that the O^+ emission does not arise from a mechanism which depends on the total energy deposited into electronic excitation. For instance, if the O^+ emission were being caused by secondary electrons via ESD, one might expect $I(O^+)$ to scale as the secondary-electron yields, which in turn are proportional to the electronic stopping power.[29] Lindhard's electronic stopping power,[31] however, depends on the projectile and target atomic numbers Z_1 and Z_2 as

$$Z_1^{7/6}/(Z_1^{2/3}+Z_2^{2/3})^{3/2}\ .$$

This factor ranges from 0.332 for Ne^+ beams to 0.805 for Kr^+ beams (both incident on Ti), an increase by a factor of 2.4 which is not reflected in our measured yields of O^+ from bombardment of O/Ti.

The O^+ yields from ion bombardment of O/Nb are shown in Fig. 2(b). The plotted yields and the fit parameters tabulated in Table I show that the yields are collinear for Ar^+ and Kr^+ beams as functions of beam velocity; however, the yields for the Ne^+ beams do not coincide with the yields for the other beams. Dividing the O^+ yields by the Lindhard electronic stopping power constant, as plotted in Fig. 9, decreases the apparent order in the data. Also, the scaled yields for different beams are not parallel, as shown by the scaled slopes presented in Table II. Although the ratios of $dI(O^+)/dv$ to $dI(e^-)/dv$ (Table II), where $I(e^-)$ is the measured secondary electron yield, are consistent for different beams, this consistency is not as compelling as that found for the Mo data (discussed in the following). Therefore, given the scatter in our data, it is perhaps reasonable to group O/Nb with O/V and O/Ti as a system for which $I(O^+)$ is proportional to projectile velocity, with the Ne^+ data being a special case for O/Nb. It must be noted that Nb and V are in the same column of the periodic table.

Comparison of Fig. 2(a) with Fig. 3(a), along with consideration of the velocity fit parameters in Table I, demonstrates that $I(O^+)$ for ion bombardment of O/Mo does depend on beam species. The Mo data divided by Lindhard's electronic stopping power constant are shown in Fig. 10(a). The scaled yields for the Ar^+ and Kr^+ beams are collinear, while the scaled yields for the Ne^+ beams are higher than, but parallel to (see Table I), those for the Ar^+ and Kr^+ beams. The agreement between the ratios of $dI(O^+)/dv$ to $dI(e^-)/dv$ for the different beams is notable, and to be contrasted with the lack of agree-

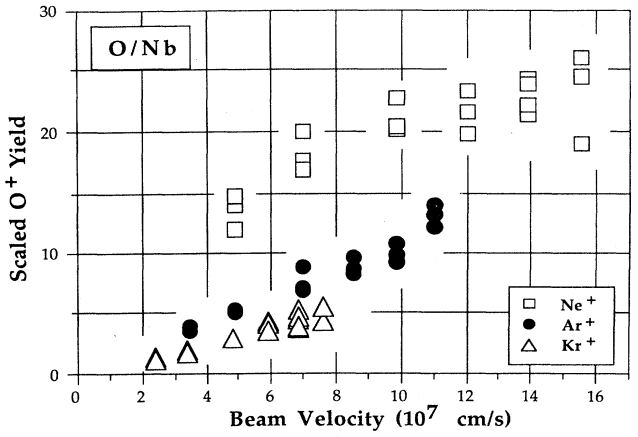

FIG. 9. Yields of O^+ from bombardment of O/Nb, divided by the beam-dependent factor in Lindhard's electronic stopping power.

TABLE II. Ratios of the computed slopes for the O^+ yields (Table I) to the slopes for the secondary electron yields (also Table I) and to the beam-dependent factor of the proportionality constant from Lindhard's electronic stopping power (as discussed in the text). Units are the same as for Table I.

Target	Beam	O^+ slope / electron slope	O^+ slope / Lindhard factor
Ti	Ne^+	2.1 ±0.4	1.2 ±0.2
	Ar^+	1.1 ±0.2	0.86 ±0.10
	Kr^+	0.75 ±0.12	0.57 ±0.06
Mo	Ne^+	1.0 ±0.1	1.2 ±0.1
	Ar^+	1.0 ±0.1	1.30 ±0.09
	Kr^+	1.1 ±0.1	1.05 ±0.07
Nb	Ne^+	0.57 ±0.11	0.70 ±0.12
	Ar^+	0.70 ±0.12	1.1 ±0.1
	Kr^+	0.61 ±0.06	0.69 ±0.05
W	Ne^+	0.23 ±0.02	0.35 ±0.03
	Ar^+	0.43 ±0.03	0.77 ±0.05
	Kr^+	0.59 ±0.09	0.64 ±0.08

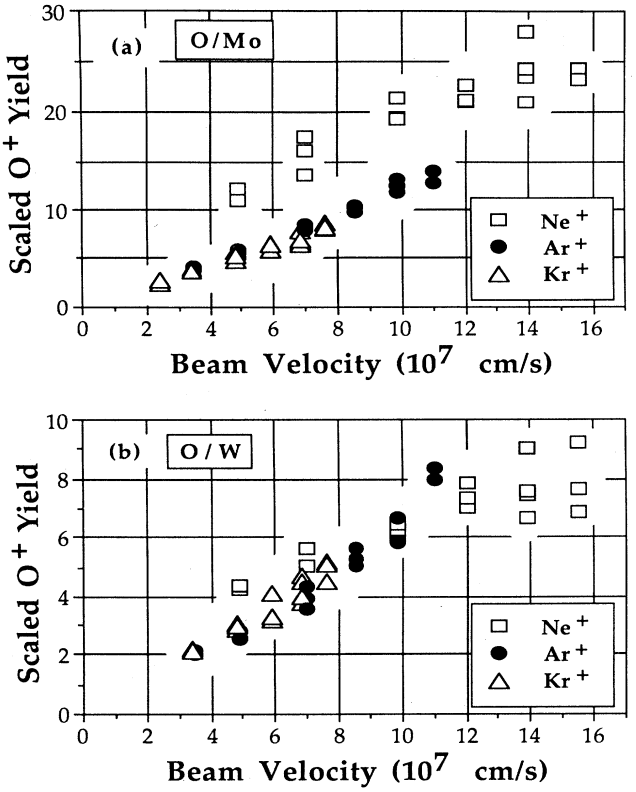

FIG. 10. Yields of O^+, divided by the beam-dependent factor in Lindhard's electronic stopping power, from bombardment of (a) O/Mo; (b) O/W.

ment for the O/Ti targets. Evidently, although Ti, V, Nb, and Mo are all transition metals in the same region of the periodic table and the yields of O^+ depend only on beam velocity for ion bombardment of O/Ti, O/Nb, and O/V,[11] the yields of O^+ from ion bombardment of O/Mo can be directly related to the yield of secondary electrons and the electronic stopping power. Therefore, the details of the O^+ emission during ion bombardment of transition metal surfaces are different for different columns of the periodic table. Moreover, in the case of O/Mo there is direct support for the suggestion[11] that the O^+ emission is caused by secondary electrons.

One feature in common for O/Nb and O/Mo under Ne^+ bombardment is the large offset of $I(O^+)$ from being strictly proportional to the projectile velocity. For both targets, we found that $I(e^-)$ also is offset for Ne^+ beams. Indeed, the ratios of the O^+ offset to the electron offset are equal for Mo and Nb (2.63±0.80 for Mo and 2.68±0.65 for Nb, both in units of 10^{-7} O^+/electron). These results suggest that there exists a mechanism for O^+ emission produced by Ne^+ bombardment, in addition to the velocity-proportional mechanism, which is related to the emission of secondary electrons. However, although for O/Ti targets $I(O^+)$ is not offset for any beam, $I(e^-)$ is offset for both the Ne^+ and the Ar^+ beams. This suggests that the equality of the offset ratios for O/Mo and O/Nb is coincidence and poses difficulties for any speculation about the existence of an additional mechanism for O^+ emission during Ne^+ bombardment.

The O^+ yields from ion bombardment of O/W [plotted in Fig. 3(b)] and the fit parameters (Table I) show that $dI(O^+)/dv$ varies strongly with beam species for this target. Dividing by the Lindhard factor [Fig. 10(b) and Table II] reduces the spread between $I(O^+)$ for the different beams, although, unlike the results for Mo, the scaled slopes and the ratios of $dI(O^+)/dv$ to $dI(e^-)/dv$ (Table II) are consistent only for Ar^+ and Kr^+, and even that consistency is not notable.

The offset of $I(O^+)$ for Ne^+ bombardment of O/W is smaller than that for O/Mo or O/Nb, although $I(e^-)$ is comparable for all three targets. Also, unlike the case for O/Mo and O/Nb, subtracting the offset would decrease the apparent order in the data. Therefore, if the additional mechanism already discussed for O^+ emission during bombardment by Ne^+ does indeed exist, it is dependent on the target used.

Given the scatter in our data for each beam, we may group the targets discussed so far into two categories. The first consists of O/V, O/Ti, and O/Nb. Here, $I(O^+)$ is strictly proportional to projectile velocity. The second group consists of O/Mo and O/W, for which $I(O^+)$ follows the electronic excitation as a function of projectile velocity. Since Mo and W are in the same column of the

periodic table, this grouping is not surprising. For both groups, however, the data for the Ne^+ beams pose difficulties for these simple characterizations of the behavior of $I(O^+)$.

Unlike the systems we have discussed so far, ion bombardment of O/Ni appears to yield O^+ emission from collision cascades rather than from electronic processes. Although the O^+ yields from bombardment of O/Ni (shown in Fig. 5) do not exactly follow the Ni^+ yields as functions of beam energy, they certainly do not increase linearly with beam velocity. This result, although expected from the maximal-valency requirement of the Knotek-Feibelman description of ESD,[8] is somewhat surprising since other workers have actually observed ESD of O^+ from O/Ni.[16–18] However, our result may be consistent with reported ESD yields. Gerritsen[18] found the total ESD yield of oxygen from O/Ni to be about 2×10^{-8} atoms/electron. Since ions typically constitute less than 10% of the total ESD yield,[32] this corresponds to an ion yield of less than 2×10^{-9} O^+/electron, which is a factor of about 10^{-3} smaller than the ESD yields typically found for maximally valent targets, such as O/Ti.[32] Therefore, the secondary-electron-induced yield of O^+ from ion bombardment of O/Ni might be expected to be less than that from O/Ti by about the same factor. Comparing our observed ion-induced O^+ yields from O/Ti with those from O/Ni, however, we see that the yields from O/Ni (presumably from collision cascades) are actually smaller than those from O/Ti by a factor of only 10^{-2}. Therefore, it is possible that the yields of any O^+ desorption induced by electronic processes are too small to be observable above the O^+ emission from collision cascades for ion bombardment of O/Ni.

B. Calculations using secondary electron distributions

If secondary electrons indeed cause the emission of O^+, then the cross section for ion-induced O^+ emission must be consistent with the integral of the energy distribution of the secondary electrons multiplied by the cross section for electron-stimulated desorption. Therefore, we used the secondary-electron energy distribution for 200 keV Ar^+ bombardment of O/V, shown in Fig. 4, to estimate the O^+ yield expected from secondary-electron-induced desorption. (Although the size of the beam spot precluded good energy resolution, this spectrum should be useful for estimating the yields.) We approximated the functional dependence on electron energy of the observed ESD yields[33] Y_{ESD} as increasing linearly from threshold at 30 eV to $Y_{\max}$ at 90 eV and remaining at $Y_{\max}$ for larger electron energies. Then, the expected measured yield of O^+ desorbed by secondary electrons during ion bombardment is

$$Y(O^+)=\gamma_e T\sum_{E_e}(Y_{\mathrm{ESD}}\cdot Y_e)\Big/\sum_{E_e}Y_e\ ;$$

both summations are over electron energy E_e. Here, γ_e is the total secondary electron yield, as determined by comparing the incident ion beam current with that measured without the collection of secondary electrons by the Faraday cage, and Y_e is the secondary-electron energy distribution shown in Fig. 4. Although the transmission T was shown above to be about 10^{-5}, T was probably larger for O^+ ions, since, using the energy distributions found by Weng for ESD from O/Ti,[34] we estimate that about one half of the O^+ emitted had energy within the energy range of our prefilter. Therefore, it seems reasonable to approximate T as 10^{-4}. The result of the calculation of $Y(O^+)$ is that the expected yield of O^+ from 200 keV Ar^+ bombardment of O/V is

$$Y(O^+)=0.53TY_{\max}\ ;$$

since $Y_{\max}$ is typically of the order 10^{-6}–10^{-5} O^+/electron,[32,35] we conclude that the expected yield is about $T\times10^{-6}$ O^+/ion. For comparison, the observed yield from O/V is about 2.5×10^{-7} O^+/ion,[11] so that, if we assume that T was 10^{-4}, the observed yield seems to have been larger by three orders of magnitude than that calculated for secondary-electron-induced desorption. Nevertheless, it must be noted that, given the results from O/Ni already discussed, the behavior of $I(O^+)$ does seem to correlate with whether the target is maximally valent, as expected from the theory of ESD;[8] this correlation would be difficult to explain with a mechanism that did not invoke some form of electronic excitation.

Since the yield and energy of ion-induced Auger electrons depend on the beam-target combination,[29,36] we further estimated the relative contribution of Ar Auger electrons to the O^+ yield estimated above in an attempt to determine whether part of the dependence of the O^+ yield on beam species could result from projectile Auger electrons. The calculations were performed in the manner already described, except that only the effect of the Auger feature near 200 eV (with background properly subtracted; see Fig. 4) was considered. Since relative yields are of interest here, the quadrupole transmission cancels out of the calculation. The calculated fraction of the O^+ yield that is due to Ar Auger electrons ranges from 6% for 50 keV beams to 15% for 200 keV beams. This additional yield is of the same order as the scatter in our data, so it is difficult to ascribe significance to it. However, similar measurements and calculations should be made for Ne^+ and Kr^+ beams, as well as for other targets.

Since the energy prefilter on our mass spectrometer sampled only a narrow range of O^+ energies, a shift in the energy distribution of the O^+ with beam energy could have produced systematic errors in the measured yields of O^+ as functions of beam velocity. Such a shift is possible, since Weng has shown that the width and the energy of the maximum of the O^+ energy distribution for ESD from O/W change with incident electron energy,[34] and the energy distribution of the secondary electrons varies with ion beam energy.[29] Using the same behavior of the ESD cross section as above and assuming that the tail of the secondary electron distribution decreases as E^{-n} ($1.5\le n\le3.0$),[37] we have calculated the maximum change in ion yield to be less than 4% over the full range of n. Given that n may not actually vary over that full range for our range of beam energies, this sets an upper limit on the systematic error introduced by the limited energy range of the prefilter during our measurements.

C. CO adsorption

The similarity between the dependences of the CO^+ yields and the metal ion yields on beam energy, shown in Fig. 7, is compelling evidence that CO^+ ions are produced by collision cascades, despite the fact that CO^+ is also observed in ESD experiments.[38] Craig[38] reports that the ESD yield of CO^+ from CO/Ni is 0.4 times that of O^+, while our CO^+ yield is 0.1 times our O^+ yield. It may be significant that our targets were exposed to 2000 L (1 L$=10^{-6}$ Torr$\times$s) of CO, in contrast to the 3 L exposure used by Craig. Also, Craig bombarded his targets with 400-eV electrons, which would correspond to the tail of the secondary-electron energy distribution. Therefore, it is possible that this discrepancy in the relative yields results from variation with electron energy of the ratio of the ESD cross section for CO^+ emission to that for O^+ emission. The energy range of our prefilter could also have produced error in the relative yields, if the energy distribution of the emitted Ni^+ was different for the two adsorbates.

The O^+ emission from ion bombardment of CO/Ni and CO/Pd, shown in Fig. 6, does not appear to originate from collision cascades. The behavior of $I(O^+)$ as a function of beam velocity also differs from that found for O/Ti, O/Nb, O/Mo, and O/W. Although the O^+ yields from Ar^+ and Kr^+ bombardment generally increase with beam velocity, the Ar^+ data for the CO/Ni target begin to decrease in the upper portion of the measured velocity range. $I(O^+)$ for Ne^+ bombardment bears no resemblance to that found for O/Ti, O/Nb, O/Mo, and O/W. These differences between the behavior of $I(O^+)$ for CO adsorption and O_2 adsorption do not arise from any peculiar behavior of the secondary-electron yields, since we found that the behavior of the secondary-electron yields for the CO-adsorbed targets resembles that found for the O_2-adsorbed targets.

For CO/Ni, the O^+ yields from Ar^+ and Ne^+ bombardment appear to lie on a common curve as functions of projectile velocity, but the yields from Kr^+ bombardment are twice as large. In Fig. 11(a), we plot these yields divided by Lindhard's electronic stopping power constant; there, the Ar^+ and Kr^+ data fall on a common curve, with the Ne^+ data twice as large. The O^+ yields from ion bombardment of CO/Pd [Fig. 6(b)] exhibit less order than those for CO/Ni. Also, the Ne^+ data are nearly independent of beam velocity and the Ar^+ data do not exhibit the maximum found for the corresponding data for the CO/Ni target. However, division by Lindhard's constant diminishes the variation with beam species somewhat, as seen in Fig. 11(b). Thus, the results for the two CO-adsorbate systems are dissimilar to one another as well as to the O_2-adsorbate systems studied, although the behavior for CO/Pd resembles that for the O_2-adsorbate systems more nearly than does the behavior for CO/Ni. We note also that comparison of the scale of Fig. 6(a) to the scale of Fig. 5(a) reveals that we observe O^+ yields from ion bombardment of CO/Ni that are ten times those from O/Ni, although Madden found the ESD yields of O^+ from O/Ni to be much larger than those from CO/Ni.[16]

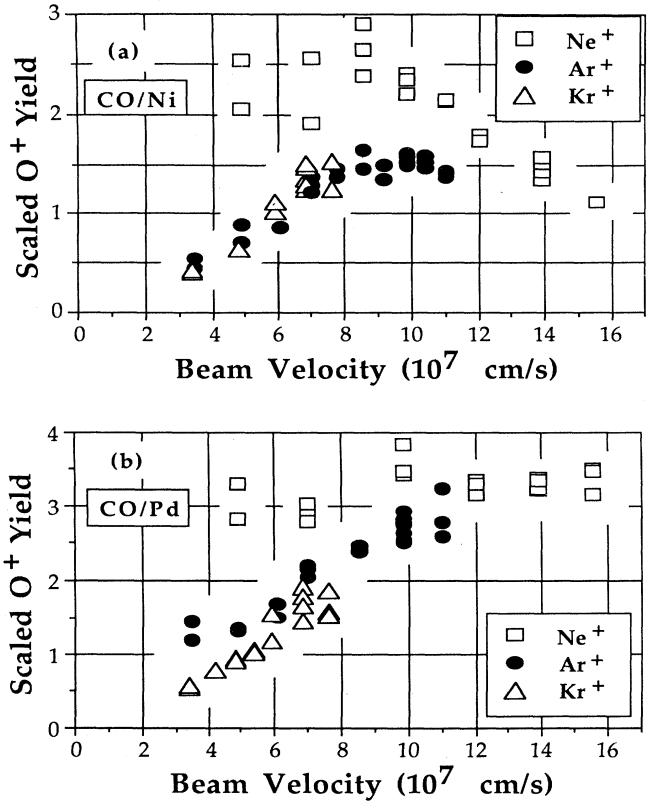

FIG. 11. Yields of O^+ divided by the beam-dependent factor of Lindhard's electronic stopping power for bombardment of (a) CO/Ni; (b) CO/Pd.

V. CONCLUSIONS

We have found that the dependence of the O^+ yields on beam velocity for ion bombardment of adsorbates on metal surfaces varies with substrate and adsorbate. Although our results for O/Ti reproduce the simple linear dependence on velocity, independent of beam species, found by Blauner and Weller for O/V,[11] our results for O/Mo exhibit a dependence on electronic stopping power. Our results for O/Nb and O/W cannot be so easily described (primarily because of the difficulties posed by the Ne^+ data), although those for O/Nb resemble those for O/Ti, while our results for O/W resemble those for O/Mo.

For ion bombardment of O_2 adsorbed onto all metals studied except Ni, the O^+ yields for each beam increase linearly with velocity, as do the results of Blauner and Weller,[11–13] suggesting that electronic processes are, in some way, involved in the O^+ emission for all of these targets. However, the magnitudes of the observed O^+ yields are not consistent with those expected if secondary electrons were producing the O^+ emission, and only the results for O/Mo exhibit a clear correlation with the secondary-electron yields in terms of the dependence on the projectile species and velocity. Although the observed O^+ yields for ion bombardment of O/Ni are consistent with emission produced by collision cascades, this

could be the result of a small ESD cross section for this system. Thus, the behavior of $I(O^+)$ does appear to correlate with that expected from the maximal-valency arguments of ESD theory, which implicates some form of electronically stimulated desorption.

We must note, however, that studies of the oxidation of titanium have produced conflicting results about the stoichiometry of the oxide formed for O_2 exposures similar to ours, with some studies suggesting that the oxide is not maximally valent.[39] If our oxide surfaces were not maximally valent, our results would have to be considered in light of findings that the ESD yield of O^+ from TiO_2 reduced by ion bombardment is larger than that from the original TiO_2.[15] Studies of ion-induced emission of O^+ from well-characterized oxide surfaces would help to clarify this point.

The O^+ emission from the covalent systems, CO/Ni and CO/Pd, does not result from collision cascades. However, the velocity dependence of the yields differs from that of the (ionic) oxidized targets.

Experiments using other transition metals, including those which form nonmaximally valent oxides, would help map out the details of the behavior of the O^+ emission. Moreover, the apparent offset of the O^+ yields during Ne^+ bombardment should be further investigated by using lower beam energies to determine whether the yields remain a linear function of beam velocity for the lower beam velocities. Experiments using the same mass spectrometer setup for both electron- and ion-induced desorption would eliminate the spectrometer's transmission from the calculation of the yields expected for secondary-electron-induced emission, as well as provide accurate measurements of the ESD yields for our target surfaces. Studies of the O^+ yields for bombardment of CO adsorbed onto such targets as Ti and W would help determine whether the behavior of the yields for CO adsorption is produced by the substrate or by the adsorbate. Investigation of the energy distribution of O^+ emitted during ion bombardment, and comparison with the energy distributions for ESD, would help to determine whether ESD processes indeed play a role in the ion-induced emission of O^+. Finally, measurements of the coincidence between O^+ emission and Auger electron emission could reveal the electronic processes occurring during the desorption.[40]

ACKNOWLEDGMENTS

This work was supported by the U.S. Department of Energy under Contract No. DE-AC02-76ER03074 and a Cottrell Research Grant from the Research Corporation. We wish to thank M. R. Weller, P. G. Blauner, L. M. Baumel, K. M. Hubbard, and P. D. Parker for assistance with these experiments and useful discussions, and D. A. Bromley for his support. We also wish to thank V. Henrich and members of the Chemistry and Materials Science Divisions of Argonne National Laboratory for their valuable comments on our work.

*Present address: Physics Department, Augustana College, Rock Island, IL 61201.

[1]G. Blaise and A. Nourtier, Surf. Sci. **90**, 495 (1979).
[2]P. Williams, Surf. Sci. **90**, 588 (1979).
[3]K. Wittmaack, in *Inelastic Ion-Surface Collisions,* edited by N. H. Tolk, J. C. Tully, W. Heiland, and C. W. White (Academic, New York, 1979), p. 153.
[4]P. Williams, Appl. Surf. Sci. **13**, 241 (1982).
[5]M. Yu and N. Lang, Nucl. Instrum. Methods **B14**, 403 (1986).
[6]M. Yu, Nucl. Instrum. Methods **B15**, 151 (1986).
[7]P. Williams, Phys. Rev. B **23**, 6187 (1981).
[8]M. L. Knotek and P. Feibelman, Phys. Rev. Lett. **40**, 964 (1978).
[9]J. O'Connor, P. Blauner, and R. Weller, Nucl. Instrum. Methods **B13**, 338 (1986).
[10]J. O'Connor, Ph.D. thesis, Yale University, 1986 (unpublished).
[11]P. Blauner and R. Weller, Phys. Rev. B **35**, 1485 (1987).
[12]P. Blauner and R. Weller, Phys. Rev. B **35**, 1492 (1987).
[13]P. Blauner, Ph.D. thesis, Yale University, 1987 (unpublished).
[14]D. P. Woodruff *et al.*, Surf. Sci. **104**, 282 (1981).
[15]R. Kurtz, R. Stockbauer, and T. Madey, in *Desorption Induced by Electronic Transition: Diet II,* edited by W. Brenig and D. Menzel (Springer-Verlag, New York, 1985), p. 89.
[16]H. H. Madden, J. Vac. Sci. Technol. **13**, 228 (1976).
[17]H. Niehus and W. Losch, Surf. Sci. **111**, 344 (1981).
[18]H. C. Gerritsen, M. P. Bruijn, J. Verhoeven, and M. J. van der Wiel, Surf. Sci. **139**, 16 (1984).
[19]M. Barber, J. C. Vickerman, and J. Wolstenholme, Surf. Sci. **68**, 130 (1977).
[20]A. Zangwill, *Physics at Surfaces* (Cambridge University Press, Cambridge, 1988), Chap. 9.
[21]M. L. Knotek and P. Feibelman, Surf. Sci. **90**, 78 (1979).
[22]D. E. Ramaker, in *Desorption Induced by Electronic Transitions: DIET I,* edited by N. H. Tolk, M. M. Traum, J. C. Tully, and T. E. Madey (Springer-Verlag, New York, 1983), p. 70, and references therein.
[23]N. Matsunami *et al.*, At. Data Nucl. Data Tables **31**, 1 (1984).
[24]Ralph Olson (private communication).
[25]A. Benninghoven, Surf. Sci. **53**, 596 (1975).
[26]P. H. Dawson, in *Quadrupole Mass Spectrometry and Its Applications,* edited by P. H. Dawson (Elsevier Scientific, New York, 1976), p. 9.
[27]*UTI100C Operation and Service Manual* (Uthe Technology International Sunnyvale California, 1979).
[28]K. J. Snowdon and R. J. MacDonald, Int. J. Mass. Spectrom. Ion Phys. **28**, 233 (1978).
[29]N. Benazeth, Nucl. Instrum. Methods **194**, 405 (1982).
[30]N. Winograd, as discussed in P. Williams, Appl. Surf. Sci. **13**, 241 (1982).
[31]J. Lindhard and M. Scharff, Phys. Rev. **124**, 128 (1961).
[32]M. L. Knotek, Rep. Prog. Phys. **47**, 1499 (1984).
[33]P. Feibelman and M. L. Knotek, Phys. Rev. B **18**, 6531 (1978).
[34]S.-L. Weng, Phys. Rev. B **23**, 1699 (1981).
[35]P. Redhead, Can. J. Phys. **42**, 886 (1964).
[36]R. Baragiola, Radiat. Eff. **61**, 47 (1982).
[37]D. Hasselkamp, S. Hippler, and A. Scharmann, Nucl. Instrum. Methods **B18**, 561 (1987).
[38]J. H. Craig, Jr., Surf. Sci. **134**, 745 (1983).
[39]A. Carley, P. Chalker, J. Riviere, and M. W. Roberts, J. Chem. Soc. Faraday Trans. 1 **83**, 351 (1987).
[40]M. L. Knotek and J. W. Rabalais, in *Desorption Induced by Electronic Transitions: Diet II,* edited by W. Brenig and D. Menzel (Springer-Verlag, New York, 1985), p. 77.